J|A|C|S
ARTICLES
Published on Web 06/21/2002

Distance Dependence of Electron Transfer in Rigid, Cofacially Compressed, π-Stacked Porphyrin−Bridge−Quinone Systems

Youn K. Kang, Igor V. Rubtsov, Peter M. Iovine, Jianxin Chen, and Michael J. Therien*

Contribution from the Department of Chemistry, University of Pennsylvania, Philadelphia, Pennsylvania 19104-6323

Received November 8, 2001. Revised Manuscript Received February 13, 2002

Abstract: The electron-transfer (ET) dynamics of a series of unusually rigid π-stacked porphyrin−quinone (P−Q) systems, in which sub-van der Waals interplanar distances separate juxtaposed porphyryl, aromatic bridge, and quinonyl components of these assemblies, are reported. The photoinduced charge separation (CS) and thermal charge recombination (CR) ET reactions of [5-[8′-(2″,5″-benzoquinonyl)-1′-naphthyl]-10,20-diphenylporphinato]zinc(II) (**1a-Zn**), [5-[8′-(4″-[8‴-(2⁗,5⁗-benzoquinonyl)-1‴-naphthyl]-1″-phenyl)-1′-naphthyl]-10,20-diphenylporphinato]zinc(II) (**2a-Zn**), and [5-(8′-[4″-(8‴-[4⁗-(8⁗⁗-[2⁗⁗,5⁗⁗-benzoquinonyl]-1⁗⁗-naphthyl)-1⁗-phenyl]-1‴-naphthyl)-1″-phenyl]-1′-naphthyl)-10,20-diphenylporphinato]zinc(II) (**3a-Zn**) in CH_2Cl_2 were investigated by pump−probe transient absorption spectroscopy. Analyses of these data show that the phenomenological ET distance dependence (β) for both the CS and CR reactions in these systems is soft ($\beta_{CS} = 0.43$ Å^{-1}; $\beta_{CR} = 0.35 \pm 0.16$ Å^{-1}). This work demonstrates that simple aromatic building blocks such as benzene, which are characterized by highly stabilized filled molecular orbitals and large HOMO−LUMO gaps, can provide substantial D−A electronic coupling when organized within a π-stacked structural motif that features a modest degree of arene−arene interplanar compression.

Introduction

Focused experimental efforts over the past several years have provided considerable mechanistic insight into the nature of electronic coupling mediated by DNA-based oligonucleotide scaffolds,[1−14] which typically feature nucleobase−nucleobase interplanar separations corresponding to van der Waals contact distances (~3.5 Å). In contrast to the rapidly expanding body of information regarding double-helical DNA-mediated electron-transfer (ET) reactions, relatively little is known regarding such reactions in other classes of π-stacked structures.

We have synthesized several examples of *unusually* rigid π-stacked porphyrin−quinone (P−Q) systems via an approach that exploits metal-catalyzed cross-coupling methodologies,[15−21] porphyryl boronate synthons,[22] and a 1,8-naphthyl[23,24] pillaring motif; these donor−spacer−acceptor (D−Sp−A) compounds define a new class of porphyrin-based supramolecular structures in which sub-van der Waals interplanar separations between juxtaposed porphyryl, aromatic bridge, and quinonyl components of these assemblies are strictly enforced.[25,26]

* To whom correspondence may be sent. E-mail: therien@a.chem.upenn.edu.

(1) Purugganan, M. D.; Kumar, C. V.; Turro, N. J.; Barton, J. K. *Science* **1988**, *241*, 1645−1649.
(2) Murphy, C. J.; Arkin, M. R.; Jenkins, Y.; Ghatlia, N. D.; Bossmann, S. H.; Turro, N. J.; Barton, J. K. *Science* **1993**, *262*, 1025−1029.
(3) Arkin, M. R.; Stemp, E. D. A.; Holmlin, R. E.; Barton, J. K.; Hörmann, A.; Olson, E. J. C.; Barbara, P. F. *Science* **1996**, *273*, 475−480.
(4) Kelley, S. O.; Jackson, N. M.; Hill, M. G.; Barton, J. K. *Angew. Chem., Int. Ed.* **1999**, *38*, 941−945.
(5) Wan, C. Z.; Fiebig, T.; Kelley, S. O.; Treadway, C. R.; Barton, J. K.; Zewail, A. H. *Proc. Natl. Acad. Sci. U.S.A.* **1999**, *96*, 6014−6019.
(6) Lewis, F. D.; Wu, T.; Zhang, Y.; Letsinger, R. L.; Greenfield, S. R.; Wasielewski, M. R. *Science* **1997**, *277*, 673−676.
(7) Lewis, F. D.; Liu, X.; Miller, S. E.; Wasielewski, M. R. *J. Am. Chem. Soc.* **1999**, *121*, 9746−9747.
(8) Lewis, F. D.; Liu, X.; Liu, J.; Miller, S. E.; Hayes, R. T.; Wasielewski, M. R. *Nature* **2000**, *406*, 51−53.
(9) Lewis, F. D.; Wu, T.; Liu, X.; Letsinger, R. L.; Greenfield, S. R.; Miller, S. E.; Wasielewski, M. R. *J. Am. Chem. Soc.* **2000**, *122*, 2889−2902.
(10) Lewis, F. D.; Kalgutkar, R. S.; Wu, Y.; Liu, X.; Liu, J.; Hayes, R. T.; Miller, S. E.; Wasielewski, M. R. *J. Am. Chem. Soc.* **2000**, *122*, 12346−12351.
(11) Meade, T. J.; Kayyem, J. F. *Angew. Chem., Int. Ed. Engl.* **1995**, *34*, 352−354.
(12) Meggers, E.; Kusch, D.; Spichty, M.; Wille, U.; Giese, B. *Angew. Chem., Int. Ed.* **1998**, *37*, 460−462.
(13) Meggers, E.; Michel-Beyerle, M. E.; Giese, B. *J. Am. Chem. Soc.* **1998**, *120*, 12950−12955.
(14) Fukui, K.; Tanaka, K. *Angew. Chem., Int. Ed.* **1998**, *37*, 158−161.
(15) Heck, R. F. *Acc. Chem. Res.* **1979**, *12*, 146−151.
(16) Kumada, M. *Pure Appl. Chem.* **1980**, *52*, 669−679.
(17) Negishi, E.; Luo, F. T.; Frisbee, R.; Matsushita, H. *Heterocycles* **1982**, *18*, 117−122.
(18) Stille, J. K. *Angew. Chem., Int. Ed. Engl.* **1986**, *25*, 508−524.
(19) Miyaura, N.; Suzuki, A. *Chem. Rev.* **1995**, *95*, 2457−83.
(20) DiMagno, S. G.; Lin, V. S. Y.; Therien, M. J. *J. Am. Chem. Soc.* **1993**, *115*, 2513−2515.
(21) DiMagno, S. G.; Lin, V. S. Y.; Therien, M. J. *J. Org. Chem.* **1993**, *58*, 5983−5993.
(22) Hyslop, A. G.; Kellett, M. A.; Iovine, P. M.; Therien, M. J. *J. Am. Chem. Soc.* **1998**, *120*, 12676−12677.
(23) House, H. O.; Koepsell, D. G.; Campbell, W. J. *J. Org. Chem.* **1972**, *37*, 1003−1011.
(24) Clough, R. L.; Kung, W. J.; Marsh, R. E.; Roberts, J. D. *J. Org. Chem.* **1976**, *41*, 3603−3609.
(25) Iovine, P. M.; Kellett, M. A.; Redmore, N. P.; Therien, M. J. *J. Am. Chem. Soc.* **2000**, *122*, 8717−8727.
(26) Iovine, P. M.; Veglia, G.; Furst, G.; Therien, M. J. *J. Am. Chem. Soc.* **2001**, *123*, 5668−5679.

10.1021/ja012504i CCC: $22.00

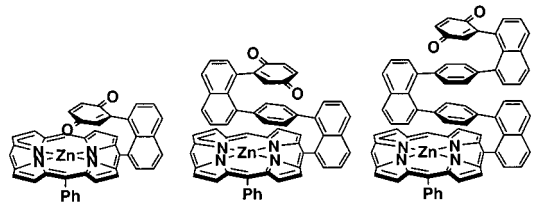

1a-Zn 2a-Zn 3a-Zn

Compounds **1a-Zn**, **2a-Zn**, and **3a-Zn** (note: in the drawings the porphyryl 20-phenyl group has been omitted for clarity) exemplify structures within this family of D−Sp−A assemblies that feature compressed, stacked π manifolds. NMR data evince that these systems display an unusual degree of conformational homogeneity in the condensed phase; furthermore, a rigorous solution NMR structural determination for the free base analogue of **2a-Zn** shows that the internuclear distances separating the C1 and C1′ carbon atoms of the 1-quinonyl and 1′-phenyl substituents of the upper naphthalene pillar, as well as the C5 and C4′ carbon atoms of the 5-porphyryl and 4′-phenyl substituents of lower naphthyl unit, correspond to 2.97 Å. These solution structural studies are thus consistent with X-ray crystallographic data which show that the separation of the C1- and C1′-phenyl carbons of 1,8-diphenylnaphthalene is 2.99 Å.[23,24]

We report herein the photoinduced electron-transfer (ET) and thermal charge recombination (CR) dynamics in **(1−3)a-Zn** and demonstrate that these structures exhibit an unusual phenomenological distance dependence for both of these classes of charge-transfer reactions.

Experimental Section

Materials. All manipulations were carried out under nitrogen prepurified by passage through an O_2 scrubbing tower (Schweizerhall R3-11 catalyst) and a drying tower (Linde 3-Å molecular sieves) unless otherwise noted. Air-sensitive solids were handled in a Braun 150-M glovebox. Standard Schlenk techniques were employed to manipulate air-sensitive solutions. All solvents utilized in this work were obtained from Fisher Scientific (HPLC grade). Tetrahydrofuran (THF) and 1,2-dimethoxyethane (DME) were dried over K/benzoylbiphenyl, while CH_2Cl_2 was dried over CaH_2; these solvents were subsequently distilled from these reagents under nitrogen. Anhydrous dimethylformamide (DMF) (Aldrich) was stirred over $MgSO_4$ prior to distillation under vacuum. Deionized water was used without any further purification. $Ba(OH)_2{\cdot}8H_2O$ (Aldrich) was recrystallized from H_2O. $Zn(OAc)_2{\cdot}2(H_2O)$ and $K_3PO_4{\cdot}nH_2O$ were used as received from Fisher Scientific. The catalyst, $Pd(PPh_3)_4$, was obtained from Strem. 1,8-Diiodonaphthalene was prepared using the procedure developed by House.[23] 1,4-Di(4′,4′,5′,5′-tetramethyl[1′,3′,2′]dioxaborolan-2′-yl)benzene was prepared via the esterification of 1,4-phenylenebisboronic acid (Aldrich) with pinacol (Aldrich) in methanol in the presence of $MgSO_4$, followed by a recrystallization from hexanes.[27] (1-Iodo-8-[4′-(8″-[2‴,5‴-dimethoxyphenyl]-1″-naphthyl)-1′-phenyl]naphthalene and [5-(4′,4′,5′,5′-tetramethyl-[1′,3′,2′[dioxaborolan-2′-yl)-10,20-diphenylporphinato]zinc(II) were prepared as reported previously.[22,25] Compounds **1a-Zn** and **2a-Zn** were prepared from their corresponding free-base porphyrin derivatives; the syntheses and characterization data for these materials have been reported previously.[25,26] Characterization and analytical data for **1a-Zn** and **2a-Zn** are available in the Supporting Information, along with the descriptions of the syntheses of [5-(8′-[4″-(8‴-[4⁗-(8⁗⁗-[2⁗⁗,5⁗⁗-dimethoxyphenyl]-1⁗⁗-naphthyl)-1⁗⁗-phenyl]-1‴-naphthyl)-1″-phenyl]-1′-naphthyl)-10,20-diphenylporphinato]zinc(II) (**3b-Zn**), 5-(8′-[4″-(8‴-[4⁗-(8⁗⁗-[2⁗⁗,5⁗⁗-benzoquinonyl]-1⁗⁗-naphthyl)-1⁗⁗-phenyl]-1‴-naphthyl)-1″-phenyl]-1′-naphthyl)-10,20-diphenylporphyrin (**3a**), and [5-(8′-[4″-(8‴-[4⁗-(8⁗⁗-[2⁗⁗,5⁗⁗-benzoquinonyl]-1⁗⁗-naphthyl)-1⁗⁗-phenyl]-1‴-naphthyl)-1″-phenyl]-1′-naphthyl)-10,20-diphenylporphinato]zinc(II) (**3a-Zn**). Chromatographic purification (Silica Gel 60, 230−400 mesh, EM Science) of all compounds was performed on the benchtop. Chemical shifts for ^{1}H NMR spectra are relative to residual protium in the deuterated solvents ($CDCl_3$, $\delta = 7.24$ ppm). All coupling constants are reported in hertz.

Instrumentation. Electronic spectra were recorded on an OLIS UV/vis/NIR spectrophotometry system that is based on the optics of a Cary 14 spectrophotometer. NMR spectra were recorded on either a 500- or 250-MHz AC-Bruker spectrometer. Mass spectral data were obtained at the University of Pennsylvania Mass Spectrometry Laboratory located within the Department of Chemistry.

Pump−Probe Transient Absorption Spectroscopic Measurements. Transient absorption spectra were obtained using standard pump−probe methods. Optical pulses, centered at 775 nm, were generated using a Ti:sapphire laser (Clark-MXR, CPA-2001). Optical parametric amplifiers (near-IR and visible OPAs, Clark-MXR) generate excitation pulses tunable in wavelength from the UV through the near-IR region; white light continuum served as the probe beam. After passing through the sample, the probe light was focused onto the entrance slit of the computer-controlled image spectrometer (SpectraPro-150, Acton Research Corp.). The baseline fluctuation in these transient absorption experiments corresponded to ~0.2 mOD per second of signal accumulation. The time resolution was probe wavelength dependent; in these experiments, the fwhm of the instrument response function varied between 140 and 200 fs. A detailed description of the transient optical apparatus will appear in an upcoming publication.[28] All experiments were carried out at room temperature (23 ± 1 °C).

Results and Discussion

Protected-quinone derivatives of **(1−3)a-Zn** ([5-[8′-(2″,5″-dimethoxyphenyl)-1′-naphthyl]-10,20-diphenylporphinato]-zinc(II) (**1b-Zn**), [5-[8′-(4″-[8‴-(2⁗,5⁗-dimethoxyphenyl)-1‴-naphthyl]-1″-phenyl)-1′-naphthyl]-10,20-diphenylporphinato]zinc(II) (**2b-Zn**), and [5-(8′-[4″-(8‴-[4⁗-(8⁗⁗-[2⁗⁗,5⁗⁗-dimethoxyphenyl]-1⁗⁗-naphthyl)-1⁗⁗-phenyl]-1‴-naphthyl)-1″-phenyl]-1′-naphthyl)-10,20-diphenylporphinato]zinc(II) (**3b-Zn**)) served as key spectroscopic benchmarks for this study. The electronic spectra of the respective singlet-excited states of these species are similar.

The photoinduced charge separation (CS) and thermal charge recombination (CR) ET dynamics of **(1−3)a-Zn** in CH_2Cl_2 were investigated by pump−probe transient absorption spectroscopy; Figure 1 displays representative data obtained for compounds **1a-Zn** and **2a-Zn**. A transient absorption near 450 nm, characteristic of the porphyrin S_1 excited state, is evident at early delay times for **2a-Zn** (Figure 1B) and **3a-Zn**; this signal is identical to that observed in the excited-state spectra of the corresponding protected-quinone derivatives of these species. In contrast, an excited-state spectrum cannot be clearly resolved for **1a-Zn**; fitting the signal observed at 700 nm (Figure 1A) as a biexponential convoluted with the instrument response function (IRF, 150 ± 5 fs) enables the magnitude of τ_{CS} to be estimated ($\tau_{CS} \leq 20$ fs).

For all three compounds, the transient absorption (~700 nm) corresponding to the (porphinato)zinc(II) cation radical is clearly

(27) Todd, M. H.; Balasubramanian, S.; Abell, C. *Tetrahedron Lett.* **1997**, *38*, 6781−6784.

(28) Rubtsov, I. V.; Kang, Y. K.; Rubtsov, G. I.; Therien, M. J. Manuscript in preparation.

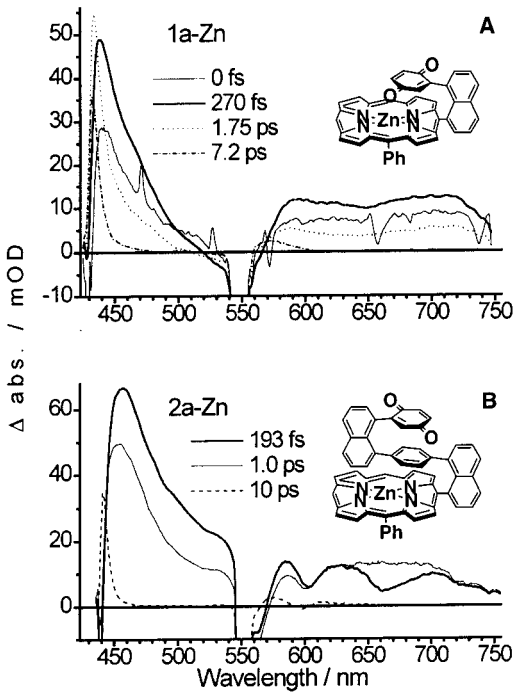

Figure 1. Transient absorption spectra of (A) **1a-Zn** and (B) **2a-Zn** in methylene chloride. Time delays are shown as insets. Experimental conditions: $\lambda_{ex} = 557$ nm, temperature $= 23 \pm 1$ °C. Note that the porphyryl 20-phenyl group has been omitted for clarity.

observed (Figure 1),[29] signaling the formation of the charge-separated state, D^+-Sp-A^-. The rate constants for CS and CR reactions were determined from a multiwavelength global fit of the visible spectral domain transient dynamics using a three-exponential function. The respective CS time constants for **2a-Zn** and **3a-Zn** were determined to be 0.62 ± 0.02 and 3.1 ± 0.3 ps; note that the observed charge-separated states for **1a-Zn**, **2a-Zn**, and **3a-Zn** undergo rapid charge recombination reactions ($\tau_{CR} = 1.6 \pm 0.2$, 1.7 ± 0.1, and 20 ± 2 ps, respectively), to produce vibrationally hot ground states. These hot ground states display characteristic absorptions at ~450 and 570 nm, and cool with a time constant of ~15 ps,[30−33] similar to that observed for strongly coupled PQ benchmarks.[30,31] Figure 2 highlights the comparative transient decay kinetics for **(1−3)a-Zn** at long wavelength ($\lambda_{ex} = 557$ nm, $\lambda_{probe} = 650$ nm), where absorptive contributions from the hot ground state are negligible.

Given that the time scales of the CS reactions in **(1−3)a-Zn** are faster or of a similar magnitude to the established anisotropy dephasing times for (porphinato)metal compounds,[30,34] pump−probe transient anisotropy studies were performed in order to establish whether electronic dephasing determines the magnitude of the electron-transfer rate constant. Figure 3 shows exemplary anisotropic transient absorption spectra obtained for **2b-Zn**. These data, and analogous spectra obtained for **1b-Zn** and

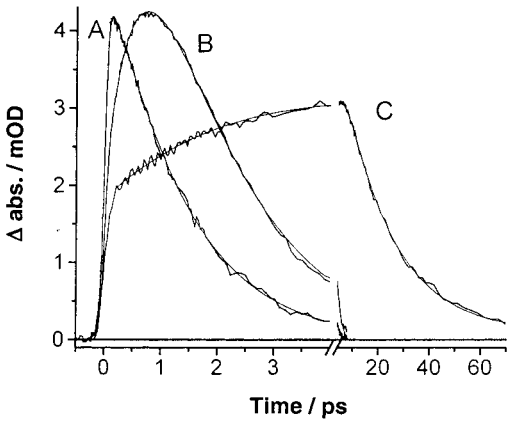

Figure 2. Transient decay kinetics determined at 650 nm for (A) **1a-Zn**, (B) **2a-Zn**, and (C) **3a-Zn**. The best biexponential function fit (convoluted in the **1a-Zn** and **2a-Zn** cases with the IRF) is depicted by the thin line (spectral contributions of the hot ground state are negligible at this wavelength). Experimental conditions: $\lambda_{ex} = 557$ nm, methylene chloride solvent, temperature $= 23 \pm 1$ °C.

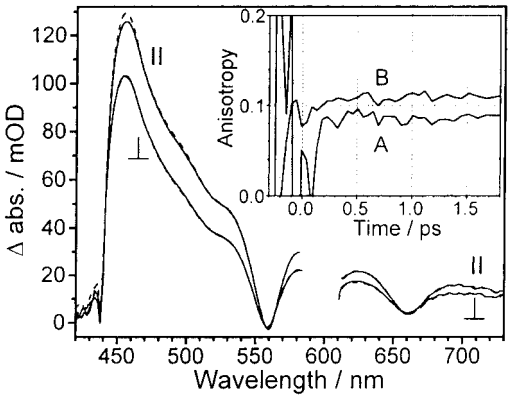

Figure 3. Anisotropic transient absorption spectra obtained for [5-[8′-(4″-[8‴-(2⁗,5⁗-dimethoxyphenyl)-1‴-naphthyl]-1″-phenyl)-1′-naphthyl]-10,20-diphenylporphinato]zinc(II) (**2b-Zn**) measured at time delays of 230 (solid lines) and 550 fs (dashed lines) for probe light polarization parallel (||) and perpendicular (⊥) to the pump pulse polarization. The inset shows (A) representative excited-state anisotropy (r) decay dynamics measured at a probe wavelength (λ_{pr}) = 700 nm and (B) the anisotropy dynamics representative of the $S_0 \rightarrow S_1$ electronic transition, which is constructed using $I_{||}'$ and $I_{\perp}'$ signal intensities for || and ⊥ polarizations, where $I_{||}' = I_{||}(531\text{ nm}) - I_{||}(558\text{ nm})$ and $I_{\perp}' = I_{\perp}(531\text{ nm}) - I_{\perp}(558\text{ nm})$. This intensity difference between the signals measured at 531 and 558 nm eliminates contributions to the anisotropy deriving from the $S_1 \rightarrow S_n$ transition, allowing estimation of the anisotropy associated with the $S_0 \rightarrow S_1$ absorption. Experimental conditions: $\lambda_{ex} = 600$ nm, methylene chloride solvent, temperature $= 23 \pm 1$ °C.

3b-Zn (data not shown), evince that the transient anisotropy dephasing times exhibited by protected-quinone compounds **(1−3)b-Zn** are <150 fs, which is the approximate fwhm of the instrument response function. No change in the magnitude of the anisotropy was observed at any recorded wavelength after a time delay of ~200 fs (Figure 3); furthermore, the magnitude of the observed anisotropy value at this time was ~0.1, which corresponds to the expected value for the doubly degenerate excited state of a pseudo-D_{4h}-symmetric (porphinato)metal compound after in-plane dephasing is complete.[30] Hence, for **(2−3)a-Zn**, excited-state electronic dephasing cannot play a role in determining the photoinduced charge separation time constant.

A variety of investigators have fit the distance dependence of nonadiabatic ET rate constants to an empirical exponential

(29) Fajer, J.; Borg, D. C.; Forman, A.; Dolphin, D.; Felton, R. H. *J. Am. Chem. Soc.* **1970**, *92*, 3451−3459.
(30) Wynne, K.; LeCours, S. M.; Galli, C.; Therien, M. J.; Hochstrasser, R. M. *J. Am. Chem. Soc.* **1995**, *117*, 3749−3753.
(31) Rodriguez, J.; Kirmaier, C.; Johnson, M. R.; Friesner, R. A.; Holten, D.; Sessler, J. L. *J. Am. Chem. Soc.* **1991**, *113*, 1652−1659.
(32) Wynne, K.; Galli, C.; Hochstrasser, R. M. *J. Chem. Phys.* **1994**, *100*, 4797−4810.
(33) Redmore, N. P.; Rubtsov, I. V.; Therien, M. J. *Inorg. Chem.* **2002**, *41*, 566−570.
(34) Galli, C.; Wynne, K.; LeCours, S. M.; Therien, M. J.; Hochstrasser, R. M. *Chem. Phys. Lett.* **1993**, *206*, 493−499.

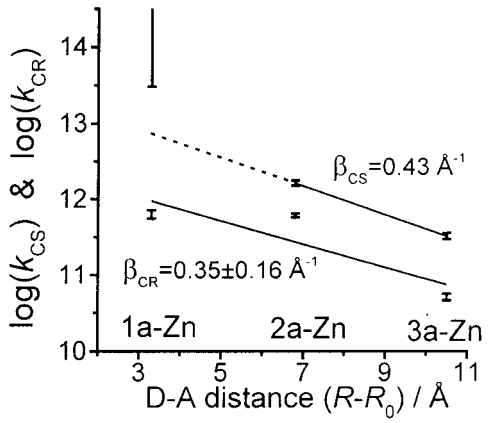

Figure 4. Distance dependence of the CS and CR rate constants for **(1−3)a-Zn** in methylene chloride at 23 ± 1 °C. Slopes of the straight line plots shown give $\beta_{CR} = 0.35 \pm 0.16$ Å^{-1} (CR) and $\beta_{CS} = 0.43$ Å^{-1} (CS) [$R_0 = 2.97$ Å; $k_0 = 1.1 \times 10^{12}$ s^{-1} (CR); $k_0 = 8.5 \times 10^{13}$ s^{-1} (CS)]. Given the adiabatic nature of CS in **1a-Zn**, β_{CS} was computed using the relevant data points for **2a-Zn** and **3a-Zn** only. Error bars for each experimental rate constant are shown. Note that the lower limit of the error bar for the CS rate constant of **1a-Zn** corresponds to the fastest rate constant that we can resolve (5×10^{13} s^{-1}); the width of this error bar is arbitrary. The error reported in β_{CR} was determined via standard linear regression analysis.

expression that reflects the expected rapid decay of electronic coupling with increasing donor (D)−acceptor (A) distance.[2,6,13,14] Figure 4 highlights the distance dependence of the CS and CR rate constants for the **1a-Zn**, **2a-Zn**, and **3a-Zn** ET systems, analyzed in terms of a simplified Marcus−Levich−Jortner equation (eq 1).[35−38] Here, the ET rate constant (k_{ET}) is assumed

$$k_{ET} = k_0 \exp[-\beta(R_{DA} - R_0)] \quad (1)$$

to be dependent upon the magnitude of the maximal rate constant at D−A contact (k_0), an exponential decay parameter (β), and the difference between the D−A separation distance (R_{DA}) and the smallest possible reactant separation (R_0), which for these systems is taken as 2.97 Å.[26] Note that because the magnitude of the ET rate constant for CS in **1a-Zn** greatly exceeds that of the fastest component of solvent relaxation ($\sim 10^{13}$ s^{-1}),[39] it was considered adiabatic and thus was not factored into our determination of β_{CS} (Figure 4).

A number of aspects of these data deserve comment. (1) Taking the extensive data set of distance- and driving force-dependent ET rate data compiled by Lewis and Wasielewski as benchmarks,[6−10] it is clear that the magnitude of the phenomenological ET distance dependence (β) for both the CS and CR reactions in these systems ($\beta_{CS} = 0.43$ Å^{-1}; $\beta_{CR} = 0.35 \pm 0.16$ Å^{-1}) is approximately a factor of 2 smaller than that determined in D/A-modified DNA hairpin structures ($\beta_{CS} = 0.7$ Å^{-1}; $\beta_{CR} = 0.9$ Å^{-1});[10] interestingly, the magnitude of these decay parameters is reminiscent of those determined for several classes of highly conjugated organic structures.[40−44] (2) Considering that the one-electron oxidation and reduction potentials (vs SCE) of benzene ($E_{1/2}^{0/+} = 2.30$ V; $E_{1/2}^{-/0} = -3.35$ V)[45,46] differ significantly from those determined for nucleobases [e.g., $E_{1/2}^{0/+}$(guanine) = 1.24 V; $E_{1/2}^{-/0}$(cytosine) = −2.42 V],[47] the comparatively soft decay of CS and CR rate constants in the **(1−3)a-Zn** series (Figure 4) with increasing D−A distance, relative to that observed for D−Sp−A assemblies based upon oligonucleotide scaffolds, is exceptional in light of the McConnell relation,[48] as the tunneling energy lies several electronvolts from the medium frontier orbitals.[49] (3) Reaction energetics[50,51] suggest that these CS and CR reactions are near barrierless only for **2a-Zn**.[52,53] This fact, coupled with the expected distance dependence of λ_S,[54−57] suggests that the pure electronic β values should be further diminished with respect to the phenomenological β_{CS} and β_{CR} values extracted from the data shown in Figure 4. (4) The magnitude of k_{CS}/k_{CR} is unusual (>60) for **1a-Zn**, given that the driving forces for CS and CR are predicted to be approximately isoergic.[52]

(35) Marcus, R. A. *J. Chem. Phys.* **1956**, *24*, 966−978.
(36) Levich, V. G. *Adv. Electrochem. Eng.* **1966**, *4*, 249.
(37) Jortner, J. *J. Chem. Phys.* **1976**, *64*, 4860−4867.
(38) Bixon, M.; Jortner, J. *Adv. Chem. Phys.* **1999**, *106*, 35−202.
(39) Reynolds, L.; Gardecki, J. A.; Frankland, S. J. V.; Horng, M. L.; Maroncelli, M. *J. Phys. Chem.* **1996**, *100*, 10337−10354.
(40) Sikes, H. D.; Smalley, J. F.; Dudek, S. P.; Cook, A. R.; Newton, M. D.; Chidsey, C. E. D.; Feldberg, S. W. *Science* **2001**, *291*, 1519−1523.
(41) Sachs, S. B.; Dudek, S. P.; Hsung, R. P.; Sita, L. R.; Smalley, J. F.; Newton, M. D.; Feldberg, S. W.; Chidsey, C. E. D. *J. Am. Chem. Soc.* **1997**, *119*, 10563−10564.
(42) Davis, W. B.; Svec, W. A.; Ratner, M. A.; Wasielewski, M. R. *Nature* **1998**, *396*, 60−63.
(43) Helms, A.; Heiler, D.; McLendon, G. *J. Am. Chem. Soc.* **1992**, *114*, 6227−6238.
(44) Osuka, A.; Maruyama, K.; Mataga, N.; Asahi, T.; Yamazaki, I.; Tamai, N. *J. Am. Chem. Soc.* **1990**, *112*, 4958−4959.
(45) Osa, T.; Yildiz, A.; Kuwana, T. *J. Am. Chem. Soc.* **1969**, *91*, 3994−3995.
(46) Meerholz, K.; Heinze, J. *J. Am. Chem. Soc.* **1989**, *111*, 2325−2326.
(47) Seidel, C. A. M.; Schulz, A.; Sauer, M. H. M. *J. Phys. Chem.* **1996**, *100*, 5541−5553.
(48) McConnell, H. M. *J. Chem. Phys.* **1961**, *35*, 508−515. The McConnell relation predicts that $\beta \propto (1/R)\ln(\Delta E/T)$, where R is the nearest-neighbor spacing, ΔE is the tunneling energy gap, and T is the nearest-neighbor electronic interaction.
(49) Lee, M.; Shephard, M. J.; Risser, S. M.; Priyadarshy, S.; Paddon-Row, M. N.; Beratan, D. N. *J. Phys. Chem. A* **2000**, *104*, 7593−7599.
(50) Marcus, R. A. *J. Chem. Phys.* **1965**, *43*, 679−701.
(51) Weller, A. *Z. Phys. Chem. N. F.* **1982**, *133*, 93−98.
(52) The Gibbs energies for charge separation (ΔG_{CS}) and charge recombination (ΔG_{CR}) were estimated using the following equations,

$$-(\Delta G_{CS}) = E_{(0,0)}(\mathrm{MP}) - E_{1/2}(\mathrm{MP/MP^+}) + E_{1/2}(\mathrm{A^-/A}) - \Delta G(\epsilon) \quad \text{(i)}$$

$$\Delta G(\epsilon) = (e^2/4\pi\epsilon_0)[(1/\epsilon_S)\{1/(2R_D) + 1/(2R_A) - 1/R_{DA}\} - (1/\epsilon_T)\{1/(2R_D) + 1/2R_A)\}] \quad \text{(ii)}$$

$$-(\Delta G_{CR}) = E_{(0,0)} + \Delta G_{CS} \quad \text{(iii)}$$

where $E_{(0,0)}$ is the energy of the lowest excited singlet state [**(1a-3a)-Zn** = 1.88, 2.05, and 2.05 eV, respectively], $E_{1/2}(\mathrm{MP/MP^+})$ is the one-electron oxidation potential of the PZn unit [**(1a-3a)-Zn** = 0.83, 0.84, and 0.82 V, respectively], $E_{1/2}(\mathrm{A^-/A})$ is the Q one-electron reduction potential [**(1a-3a)-Zn** = −0.60, −0.58, and −0.56 V, respectively], and ϵ_T is the static dielectric constant for the high-dielectric solvent in which the potentiometric measurements were obtained. The estimated energetics for these CS and CR reactions are thus ΔG_{CS}(**1a-Zn**) = −0.90 eV, ΔG_{CR}(**1a-Zn**) = −0.98 eV; ΔG_{CS}(**2a-Zn**) = −0.87 eV, ΔG_{CR}(**2a-Zn**) = −1.18 eV; ΔG_{CS}(**3a-Zn**) = −0.82 eV, ΔG_{CR}(**3a-Zn**) = −1.23 eV.

(53) The solvent reorganization energy (λ_S) and the total reorganization energy (λ_T) were calculated using

$$\lambda_S = (e^2/4\pi\epsilon_0)(\{1/(2R_D) + 1/(2R_A) - 1/R_{DA}\})[(1/\epsilon_{OP}) - (1/\epsilon_S)] \quad \text{(iv)}$$

$$\lambda_T = \lambda_S + \lambda_i \quad \text{(v)}$$

where R_D is the PZn radius (5.5 Å), R_A is the Q radius (3.2 Å), R_{DA} is the porphyrin plane-to-quinonyl centroid distance (**1a-Zn** = 3.3 Å; **2a-Zn** = 6.8 Å; **3a-Zn** = 10.5 Å), and ϵ_{OP} and ϵ_S are the optical and static dielectric constants. This analysis estimates λ_S values for **1a-Zn**, **2a-Zn**, and **3a-Zn** as 0.24, 0.96, and 1.24 eV, respectively). The total inner-sphere reorganization energy (λ_i) for **(1a−3a)-Zn** was estimated to be 0.4 eV using standard methods (see, for example: Rubtsov, I. V.; Shirota, H.; Yoshihara, K. *J. Phys. Chem. A* **1999**, *103*, 1801−1808).

(54) Tavernier, H. L.; Fayer, M. D. *J. Phys. Chem. B* **2000**, *104*, 11541−11550.
(55) Bixon, M.; Jortner, J. *J. Phys. Chem. B* **2000**, *104*, 3906−3913.
(56) Berlin, Y. A.; Burin, A. L.; Ratner, M. A. *J. Phys. Chem. A* **2000**, *104*, 443−445.
(57) Tong, G. S. M.; Kurnikov, I. V.; Beratan, D. N. *J. Phys. Chem. B* **2002**, *106*, 2381−2392.

Conclusion

In summary, we have (i) carried out the first ET experiments in π-stacked D−Sp−A systems in which sub-van der Waals interplanar distances (closest atom−atom contacts = 2.97 Å) separate juxtaposed D, Sp, and A moieties and (ii) determined the phenomenological distance dependence of the photoinduced charge separation and thermal charge recombination reactions in the species over D−A distances ranging between 3.3 and 10.5 Å (porphyrin plane to quinonyl centroid). This work shows that simple aromatic building blocks such as benzene, which are characterized by highly stabilized filled molecular orbitals and large HOMO−LUMO gaps, can provide substantial D−A electronic coupling when organized within a π-stacked structural motif that features a modest degree of arene−arene interplanar compression.

Acknowledgment. This work was supported by a grant from the Division of Chemical Sciences, Office of Basic Energy Research, U.S. Department of Energy (DE-FG02-94ER14494). M.J.T. thanks the Office of Naval Research (N00014-97-0317) and the MRSEC Program of the National Science Foundation (DMR-00-79909) for equipment grants for transient optical instrumentation.

Supporting Information Available: Optical spectra of **(1−3)a-Zn**, along with characterization data and synthetic procedures for **1a-Zn**, **2a-Zn**, **3b-Zn**, **3a**, **3a-Zn** and key naphthyl-containing precursors (PDF). This material is available free of charge via the Internet at http://pubs.acs.org.

JA012504I